IEEE Access
Multidisciplinary ⋮ Rapid Review ⋮ Open Access Journal

Received August 5, 2020, accepted August 17, 2020, date of publication August 21, 2020, date of current version September 4, 2020.

Digital Object Identifier 10.1109/ACCESS.2020.3018476

Two-Layered Model Predictive Control Strategy of the Cut Tobacco Drying Process

ANGANG CHEN[1,2], ZHENGYUN REN[1], ZHIPING FAN[1,2,3], AND XUE FENG[1]

[1]College of Information Science and Technology, Donghua University, Shanghai 201620, China
[2]Department of Chemical and Materials Engineering, University of Alberta, Edmonton, AB T6G 2G6, Canada
[3]School of Electrical and Electronic Engineering, Anhui Science and Technology University, Chuzhou 233100, China

Corresponding author: Zhengyun Ren (renzhengyun@dhu.edu.cn)

This work was supported in part by the Fundamental Research Funds for the Central Universities under Grant CUSF-DH-D-2018100, and in part by the China Scholarship Council under Grant 201806630067.

ABSTRACT In this article, a two-layered model predictive control strategy is proposed for the nonsquare system of nonlinear cut tobacco drying process. The control objective is to optimize the drum dryer temperature, hot air temperature, and cut tobacco outlet temperature meet the process constraints while meeting the moisture content of cut tobacco. Firstly, the tobacco drying process system was introduced, and the nonsquare system model and performance index function were established. Then a nonlinear moving horizon estimator (NMHE) and real-time optimization (RTO) are designed. NMHE provides state and parameter estimation for the controller, and RTO provides an optimal operating setpoint for the controller. Subsequently, a two-layered model predictive control (SSTO-MPC) design integrated with a steady-state target optimization layer (SSTO) is proposed for the nonsquare system of nonlinear cut tobacco drying process. Extensive simulations under different scenarios illustrate the effectiveness of the proposed SSTO-MPC design compared with the conventional MPC.

INDEX TERMS Cut tobacco drying process, moving horizon estimation, model predictive control, nonsquare system, steady-state target optimization, real-time optimization.

I. INTRODUCTION

The main function of the cut tobacco drying process is to reduce the moisture content in cut tobacco, which is convenient for subsequent processing and storage. As one of the largest energy consumption equipment in the industry, drying equipment accounts for about 10%−25% of industrial energy consumption [1]–[5]. Most industrial dryers are low in energy efficiency, ranging from a disappointing 10% to an acceptable 60%. Due to the rising cost of energy and the increasingly fierce global competition, energy efficiency improvement is an urgent goal for the industry. Most scientific research is still focused on understanding drying mechanism and product quality, rather than the related control of drying equipment. The cost and energy consumption of drying equipment in the industry does not lie in the initial cost investment, but the equipment's daily operation and maintenance. In order to obtain the desired product quality, the control strategy is a very critical step [6]–[11].

The classical proportional–integral–differential (PID) control is the most commonly used control strategy in the cut tobacco drying system [1], [7], [12]. Because there are more than 100 kinds of drying equipment in the world and the complexity of drying mechanisms, no controller can be applied to all drying equipment, leading to an uneven design level of drying equipment and low efficiency of most control strategies. In the literature, various control strategies have been applied to drying equipment, from internal model control (IMC) [13], fuzzy control [14] to model predictive control (MPC) [9], [15]–[18]. However, most of the control strategies are based on a linear drying process. We know that the drying process mechanism is a highly nonlinear process, and the linear model is often not enough to fully describe the process, which is also a direct reason for the low energy efficiency of drying equipment [19]. With the improvement of computer load capacity, it also promotes advanced technology (MPC) to solve nonlinear problems, continuously improve product quality specifications and energy efficiency, and make the system operate closer to the boundary of permitted operation area [20], [21]. In the traditional MPC control structure, the upper real-time optimization (RTO) bridges the gap

The associate editor coordinating the review of this manuscript and approving it for publication was Hiram Ponce.

among economic and control worlds and periodically transfers all input and output steady-state operation setpoints to the lower MPC, and the task of MPC is to transfer the system from the current state to the target state. In practice, due to the different system models used by RTO and MPC, MPC can not reach the operating setpoints of RTO optimization, resulting in a steady-state static error of system output. This is another direct reason for the low energy efficiency of drying equipment [22], [23].

The drying process of cut tobacco is a nonlinear and nonsquare system; the number of input variables is less than the number of output variables. For the nonsquare multivariable control system, the system's steady-state gain matrix is irreversible, so the steady-state value of the control input cannot be obtained from the system output setpoint value and the steady-state gain matrix, which leads to the existence of static error control in the nonsquare system. For the cut tobacco drying process's nonsquare system, the compatibility and uniqueness of input and output steady-state values are all due to RTO's unreasonable setpoint value, which leads to no solution of input and output steady-state relationship. To solve the nonsquare system control problem: (1) Reselect a set of more reasonable operation setpoints. (2) The number of steady-state equations is reduced so that the steady-state equations have unique solutions. Motivated by these considerations and inspired by Hedengren *et al.* [24], Li and Ding [25], Kassmann *et al.* [26], Liu *et al.* [27], Mao *et al.* [28], and Zhang *et al.* [29], two control strategies are proposed in cut tobacco drying process in this article. The first control strategy is two-layered model predictive control, which adds a steady-state target optimization layer (SSTO) between RTO and MPC to reselect a more reasonable set of steady-state operating setpoints. Another control strategy is zone MPC, which is to relax some system output variables' control requirements and give an allowable output interval. The purpose is to reduce the number of steady-state equations and increase the system's degree of freedom to eliminate the steady-state static error and realize the offset free control. First, the cut tobacco drying process system and its model are introduced, and the performance indices are formulated. Then, the nonlinear moving horizon estimator (NMHE) and RTO are employed to estimate the system parameters, states, and optimal operating setpoints, and the controller is designed by its ability to deal with system constraints and nonlinearity. Subsequently, a two-layered MPC based on SSTO, and zone MPC were proposed to optimize the cut tobacco drying process. The conventional RTO-MPC is also introduced for comparison purposes. The simulation results under different scenarios have demonstrated that the proposed two-layered MPC based on SSTO provides a more flexible way to handle the cut tobacco drum dryer system's optimization problem in the presence of system nonlinearities, constraints, and disturbances.

The remainder of this article is organized as follows: a detailed description of the cut tobacco drum dryer system and its fourth-order nonlinear open equation model and the performance indices function are presented in Section 2. Section 3 introduces the design of NMHE and RTO, and Section 4 and 5 provide the design details of the proposed two-layered model predictive control strategy (SSTO and MPC). Extensive simulations have been conducted in Section 6 to verify the performance of the proposed two-layered model predictive control strategy over conventional RTO-MPC in setpoint tracking and disturbance rejection. Finally, we give conclusions in Section 7.

II. SYSTEM DESCRIPTION AND PERFORMANCE INDICES

A. SYSTEM DESCRIPTION

In this work, we consider a tobacco drum dryer system with a production capacity of $500kg/min$. The schematic of the system is shown in figure 1. The drum-type drying equipment uses steam as the heating energy, adopts the conduction and convection mixed drying method to dry and dehumidify the cut tobacco, mainly conducts the heating, and supplements the convection heating. The heated steam heats the drying cylinder through the steam supply system of the dryer. The cut tobacco is fed into the continuously rotating drum by a vibrating conveyor. The drying cylinder wall is in direct contact with the cut tobacco, and the heat is transferred to the cut tobacco in a conductive manner. Simultaneously, hot air flows from the feed end to the cut tobacco in the tube. The hot air directly contacts the cut tobacco and transfers the heat to the cut tobacco through convection to enhance moisture evaporation from the cut tobacco. After the cut tobacco absorb heat from the cylinder wall and the hot air, the temperature rises, the moisture evaporates on the cut tobacco surface and diffuses into the hot airflow. The hot air flow absorbs water vapor, becomes humid and hot air, and enters the air dust box from the drying cylinder's discharge end. In the whole process, under the action of the heating cylinder wall and hot air, the cut tobacco will continue to rotate with the rotation of the inclined cylinder, and then gradually slide from the high end of the drying cylinder to the discharge end.

For computational tests in this work, it was assumed that the drum dryer is adiabatic (Heat loss Q_{l1} and Q_{l2} equal to 0) and moisture movement and heat transfer are one dimensional; has a drum length L of $7.7m$; diameter of $1.25\ m$; the slope of $3.5\ degree$; has an area A, cross-area $A1$ and the volume V. No chemical reaction takes place during drying, i.e., thermal and chemical properties of the material, air and moisture are constant within the range of temperatures considered; Drying air is distributed uniformly through the dryer. The mass flow at the drum dryer's input and output must be equal; otherwise, the system's mass and heat capacity will change.

Based on mass and energy balances, a fourth-order nonlinear model shown below can be developed to describe the dynamics of the above cut tobacco drum dryer system:

$$\rho_p V \frac{dw}{dt} = \dot{m}_{in} w_{in} - \dot{m}_{out} w - \rho_p V R_{evap} \tag{1}$$

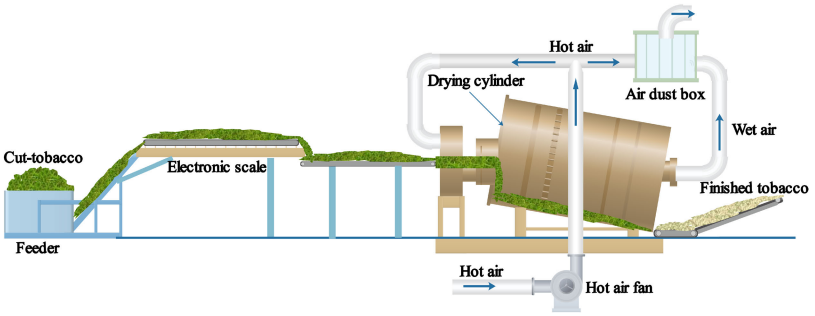

FIGURE 1. Schematic of cut tobacco drum dryer system.

$$\frac{dT_{dryer}}{dt} = \frac{\rho_{air}c_{air}q\left(T_{in}-T_{dryer}\right)}{\rho_{mix}Vc_{mix}} + \frac{\dot{m}_{in}c_p\left(T_{pin}-T_{pout}\right)}{\rho_{mix}Vc_{mix}} + \frac{\rho_pVR_{evap}c_w\left(T_{pin}-T_f\right)}{\rho_{mix}Vc_{mix}} + \frac{Akeff\left(T_{c2}-T_{dryer}\right)}{L\rho_{mix}Vc_{mix}} - Q_{l2} \quad (2)$$

$$\frac{dT_{pout}}{dt} = \frac{Akeff1\left(T_{dryer}-T_{pout}\right)}{L\rho_pVc_p} + \frac{Akeff1\left(T_1-T_{pout}\right)}{L\rho_pVc_p} - \frac{\rho_pVR_{evap}c_w\left(T_{pout}-T_{pin}\right)}{\rho_pVc_p} \quad (3)$$

$$\frac{dT_1}{dt} = \frac{\rho_{air}c_{air}q\left(T_{in}-T_1\right)}{\rho_{aw}Vc_{aw}} + \frac{A_1keff2\left(T_{c1}-T_1\right)}{L\rho_{aw}Vc_{aw}} - Q_{l1} \quad (4)$$

$$R_{evap} = 0.0001649exp\left(\frac{2T_{dryer}+T_1}{T_1}\right) \quad (5)$$

ρ_{mix} and c_{mix} are the mixing density and mixing specific heat capacity in the drum, ρ_{aw} and c_{aw} are the mixing density and mixing specific heat of air and water in the heater. $keff = 100$, $keff1 = 5$, $keff2 = 700$ are all thermal conductivity $(W/m^{\circ}C)$; here, they were considered constant along the time; in the following nonlinear dynamic estimation section, these three parameters will be estimated.

B. OPERATIONAL DATA AND PERFORMANCE INDICES

Table 1 specifies the inlet and outlet data of the dryer in operation, assuming that the speed of cut tobacco and hot air, the specific heat of tobacco, water and air, and the quality of tobacco and hot air are always constant.

TABLE 1. Inlet and outlet data of the cut tobacco dryer (operational data).

Property	Symbol	Data
Mass flow of cut tobacco (kg/min)	$\dot{m}_{in} = \dot{m}_{out}$	500
Volume flow of dry air (m^3/min)	q	2000/60
Specific heat of water liquid $(KJ/kg^{\circ}C)$	c_w	4.18
Specific heat of water vapor $(KJ/kg^{\circ}C)$	c_v	1.85
Specific heat of the dry air $(KJ/kg^{\circ}C)$	c_{air}	1.01
Specific heat of the cut tobacco $(KJ/kg^{\circ}C)$	c_p	1.83
Density of water (kg/m^3)	ρ_w	1000
Density of the air (kg/m^3)	ρ_{air}	1.293
Density of the cut tobacco (kg/m^3)	ρ_p	320
Inlet moisture content of the air	w_a	0.14
Inlet moisture content of the cut tobacco	w_{in}	0.19
Outlet moisture content of the cut tobacco	w	0.13 – 0.16
Inlet speed of the air (m/s)	v_a	0.3
Air inlet of temperature $(^{\circ}C)$	T_{in}	20
Inlet temperature of the cut tobacco $(^{\circ}C)$	T_{pin}	30
Outlet temperature of the cut tobacco $(^{\circ}C)$	T_{pout}	20 – 100
Hot air temperature $(^{\circ}C)$	T_1	100 – 120
The temperature of drum dryer $(^{\circ}C)$	T_{dryer}	130 – 170

NOTATION

c_1, c_2 and c_3 = Weights and cost.

f, g, and h = Output functions, equality and inequality constraints.

T_{c1} and T_{c2} = Control inputs.

$\hat{x}$, $\hat{y}$, $\hat{p}$ and $\hat{d}$ = The estimated values of x, y, p and d.

x_0, y_x and $\bar{y}$ = Initial state, measurements and prior model outputs.

W_m = Measurement deviation penalty.

$c_{\Delta p}$ = Penalty from the prior parameter values.

W_p = Penalty from the prior solution.

Δp^T = Change in parameters.

CV and MV = Controlled variable and manipulated variable.

y_t = Desired trajectory target $(y_{t,RTO}, y_{t,SSTO})$.

u_{LL} and u_{HL} = The lower and upper bounds of operation constraints of the control inputs.

u_{LLL} and u_{HHL} = The lower and upper bounds of engineering constraints of the control inputs.

y_{LL} and y_{HL} = The lower and upper bounds of operation constraints of the controlled variables.

y_{LLL} and y_{HHL} = The lower and upper bounds of engineering constraints of the controlled variables.

ε_1, ε_2, ε_3 and ε_4 = Slack variables.

w_1, w_2, w_3 and w_4 = The weights on the slack variables.

W_t = Penalty outside reference trajectory.

w_u and w_y = The weights on input and output.

Δu = Manipulated variable change.

$W_{\Delta u}$ = Manipulated variable movement penalty.

sp = Operating setpoint.

sp_{hi} and sp_{lo} = Upper and lower bounds to final setpoint dead-band.

τ_c = Time constant of desired controlled variable response.

w_{hi}^T and w_{lo}^T = Penalty outside reference trajectory.

e_{hi} and e_{lo} = Upper and lower error outside dead-band.

Δu_U and Δu_L = Upper and lower manipulated variable change.

$y_{t,hi}$ and $y_{t,lo}$ = Upper and lower bounds to desired trajectory target.

Two common manipulated variables are the steam temperature T_{c1} of the heater and the heating steam temperature T_{c2} of the drum dryer. Let us define the state vector as $x = \left[w\ T_{dryer}\ T_{pout}\ T_1\right]^T$, the manipulated input vector as $u = \left[T_{c1}\ T_{c2}\right]^T$, and the process output vector as $y = \left[w\ T_{dryer}\ T_{pout}\ T_1\right]^T$, a set of parameters $p = \left[keff\ keff1\ keff2\right]^T$, d is a time varying trajectory of disturbance values. output functions, equality and inequality constraints are represented by f, g, and h, respectively. Then the dynamic mathematical model of cut tobacco drum dryer system can be described by a compact nonlinear open equation form model as follows:

$$\begin{aligned} 0 &= f\left(\frac{dx}{dt}, x, y, p, d, u\right) \\ 0 &= g(x, y, p, d, u) \\ 0 &\le h(x, y, p, d, u) \end{aligned} \tag{6}$$

The real-time optimization (RTO) economic function used in the simulation is presented in equation 7. The main objective is to minimize the steam temperature T_{c1} of the heater and the heating steam temperature T_{c2} of the drum dryer, and at the same time minimize the cut tobacco outlet temperature T_{pout}.

$$J_2(u, y, c) = -c_1 w + c_2 T_{pout} + c_3(T_{c1} + T_{c2}) \tag{7}$$

The steady-state target optimization (SSTO) economic function used in the simulation is presented in equation 8. It has the same terms of RTO's economic function; hence, the same objective and an additional term are included to penalize the previous RTO setpoint's distance.

$$J_{4/5}(u, y, c) = -c_1 w + c_2 T_{pout} + c_3(T_{c1}+T_{c2}) + \|y - y_s\|_Q^2 \tag{8}$$

where u and y represent the system outputs and inputs respectively, c_1 and c_2 are the weight of the cut tobacco output moisture w and the cut tobacco outlet temperature T_{pout}, and c_3 is the cost associated with the control inputs T_{c1} and T_{c2}.

III. NONLINEAR DYNAMIC ESTIMATION AND REAL-TIME OPTIMIZATION

This section introduces nonlinear moving horizon estimator (NMHE) and real-time optimization (RTO). We propose using NMHE for states and parameter estimation purposes since it can handle nonlinear systems and take into account constraints [30]–[35]. The RTO is utilized to coordinate the network of process units and to provide optimal setpoints for the lower controllers [22], [23]. The NMHE and RTO structure considered in this work are represented in figure 2.

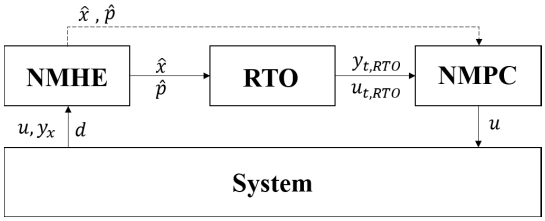

FIGURE 2. General nonlinear control structure.

A. NONLINEAR DYNAMIC ESTIMATION OF MHE

State estimation and parameter estimation have gained valuable applications in the chemical process industry by strengthening process monitoring and control. Examples of industrial applications include offline and online process system identification, online monitoring and fault detection, parameter estimation for model predictive control, and process disturbance prediction. Certain states of the system cannot often be measured directly, or the direct measurement cost is too high, which requires the estimation of these states based on the system's output measurement. For the cut tobacco drum dryer system, the measurable outputs are the hot air temperature T_1, the drum dryer temperature T_{dryer} and the cut tobacco outlet temperature T_{pout}, while the cut tobacco outlet moisture w is unmeasured. Simultaneously estimate three parameters $keff$, $keff1$ and $keff2$. In the proposed double-layer MPC design, the system's overall state and parameters are required, making the design of state and parameter estimator necessary.

MHE aims to estimate the states and parameters and readjust the predicted and measured values of the model. The model prediction matches the previous measurement results by adjusting the parameters and initial conditions of the model. As the estimation range increases, the solution's sensitivity to x_0 decreases at x_n. The only d has a significant effect on the current model state in a sufficiently long time frame. Therefore, it is usually unnecessary to estimate the initial state x_0 as the degree of freedom in the optimization problem.

$$\begin{aligned} \min_{\hat{x},\hat{y},\hat{p},\hat{d}}\ & J_1 = \left(y_x - \hat{y}\right)^T W_m \left(y_x - \hat{y}\right) + (\hat{y} - \bar{y})^T W_p (\hat{y} - \bar{y}) \\ & \quad + \Delta p^T c_{\Delta p} \\ s.t.\ & 0 = f\left(\frac{dx}{dt}, \hat{x}, \hat{y}, \hat{p}, \hat{d}, u\right) \\ & 0 = g(\hat{x}, \hat{y}, \hat{p}, \hat{d}, u) \\ & 0 \le h(\hat{x}, \hat{y}, \hat{p}, \hat{d}, u) \end{aligned} \tag{9}$$

In the above optimization equation 9, $\hat{x}$, $\hat{p}$ and $\hat{d}$ represent the estimated values of x, p and d, respectively; J_1 represents minimized objective function result; $\hat{y}$ represents model outputs $\left(\hat{y}_0 \cdots \hat{y}_N\right)^T$; y_x represents measurements $\left(y_{x,0} \cdots y_{x,N}\right)^T$; $\bar{y}$ represents prior model outputs $(\bar{y}_0 \cdots \bar{y}_N)^T$; W_m represents measurement deviation penalty; W_p represents penalty from the prior solution; $c_{\Delta p}$ represents penalty from the prior parameter values; Δp^T represents

change in parameters; N represents the size of the estimation window. The NMHE structure, as shown in figure 2 and 3, at time step k, which is based on a rigorous process model, computes the parameters and states, $\hat{x}$ and $\hat{p}$ to transmitted to RTO, SSTO and MPC.

B. DESIGN OF REAL-TIME OPTIMIZATION (RTO)

In figure 2, real-time optimization (RTO), the optimal values of setpoints are recalculated periodically (for example, hourly or daily). RTO is utilized to coordinate the process units' network and provide optimal setpoints for the lower controllers, called supervisory control. These repetitive calculations involve solving a constrained, steady-state optimization problem. The RTO optimization problem is described in equation 10. Where J_2 is the scalar economic function to be minimized, $y_{t,RTO} = L_u u_{t,RTO}$ represents the steady-state input-output linear mapping obtained by the nonlinear system; u_{LL} and u_{HL} are the lower and upper bounds of operation constraints of the control inputs, respectively; and y_{LL} and y_{HL} are the lower and upper bounds of operation constraints of the controlled variables, respectively.

$$\begin{aligned} \min_{y_{t,RTO},u_{t,RTO}} \quad & J_2 = c_y^T y_{t,RTO} + c_u^T u_{t,RTO} \\ s.t.\ & y_{t,RTO} = L_u u_{t,RTO} \\ & u_{LL} \le u_{t,RTO} \le u_{HL} \\ & y_{LL} \le y_{t,RTO} \le y_{HL} \end{aligned} \tag{10}$$

The RTO optimization algorithm's output is sent downwards to the control structure targeting the plant to the economic increase direction. Comparing the RTO and MPC models, it is clear that they are different models, so there is no guarantee that the predictions obtained through them will be consistent, unless perhaps when the process is operating close to the linearization point. Further, the inconsistency between the steady-state RTO model and the dynamic MPC model may cause the MPC regulator to produce steady-state input and output errors.

Another issue that arises when using RTO is its sampling period. As RTO optimization only starts after the process reaches a steady-state, it might happen that MPC targets will not be updated for a long time, which might reflect in economic loss. In many cases of the real world, the disturbances' dynamics are comparable with the process dynamics. Hence, the hierarchical control system should deal with fast disturbances properly.

A better option is the inclusion of the sub-layer steady-state target optimization (SSTO) to improve the integration of RTO and MPC and counteract the disadvantages just mentioned. The sub-layer is executed at the same MPC frequency and uses the steady-state version of the MPC model. Its purpose is to correct RTO setpoints to steady-state targets that are attainable by the MPC regulator. By choosing the SSTO approach, one can expect to: have a faster reaction of the control structure in response to the occurrence of disturbances, avoid giant steps in setpoint changes that might cause instability, deal with the offset from the desired targets in a more controlled and optimized way.

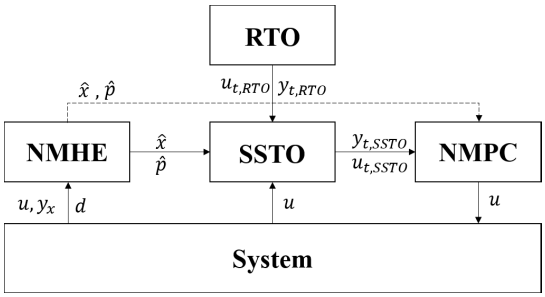

FIGURE 3. Extended control structure, considering an intermediary steady-state target optimization stage.

IV. DESIGN OF THE SUB-LAYER STEADY-STATE TARGET OPTIMIZATION (SSTO)

In this section, we introduce steady-state target optimization (SSTO). We propose using SSTO for recalculating the steady-state target value of CV and MV and realizing the asymptotic tracking of RTO calculation results [25], [26], [31]. The optimal operating setpoints of SSTO is sent downwards to the MPC control structure. SSTO and MPC structure considered in this work are represented in figure 3.

There is a real-time optimization layer (RTO) at the top of the control system, and the optimization cycle is hour level. The optimizer combines the whole process optimization index and user-defined goal to give some CV and MV ideal setpoints. However, the existence of process constraints and the influence of model mismatch or disturbance may make the system not reach the desired setpoints. The steady-state target optimization is to recalculate the steady-state target value of CV and MV (that is, the setpoints of dynamic control) at every moment of MPC controller execution. On the one hand, steady-state target optimization (SSTO) can realize the asymptotic tracking of RTO calculation results; on the other hand, it can also achieve the local economic optimization of the MPC corresponding process. Therefore, at each sampling time, the first step is to calculate the steady-state target, find steady-state operating setpoints $y_{t,SSTO}$, $u_{t,SSTO}$ in the feasible region, and make it as close to the expected values $y_{t,RTO}$, $u_{t,RTO}$ as possible.The hierarchical structure optimization control is shown in figure 3. This structure includes an intermediary layer, called steady-state target optimization (SSTO), which computes modified targets to guarantee the controllability of the MPC controller.

For a steady-state optimization problem, the optimization process can be artificially divided into two stages: (1) In the feasibility stage, to ensure that the optimization problem is feasible; (2) In the economic optimization stage, the optimization is carried out in the feasible space to find the optimal solution that makes the economic objective function optimal. First, it determines whether space (domain) formed by the constraints exists, if it exists, it will be optimized in it; if it

does not exist, it will obtain the feasible space through soft constraint adjustment, and then solve it.

A. FEASIBILITY JUDGMENT OF SSTO

The feasibility judgment of the steady-state objective optimization problem can be attributed to the following nonlinear programming problem in equation 11. where J_3 is the scalar economic function to be minimized, $f(\hat{x}, \hat{y}, \hat{p}, \hat{d}, u) = 0$ represents the nonlinear system steady-state output functions; u_{LL} and u_{HL} are the lower and upper bounds of operation constraints of the control inputs, respectively; and y_{LL} and y_{HL} are the lower and upper bounds of operation constraints of the controlled variables, respectively. u_{LLL} and u_{HHL} are the lower and upper bounds of engineering constraints of the control inputs, respectively; and y_{LLL} and y_{HHL} are the lower and upper bounds of engineering constraints of the controlled variables, respectively. ε_1, ε_2, ε_3 and ε_4 are slack variables, and w_1, w_2, w_3 and w_4 represent the weights on the slack variables. If $J_3 = 0$, it indicates that the feasible region exists, and the original SSTO problem is feasible; if $J_3 > 0$, it indicates that the feasible region does not exist, and the original SSTO problem is not feasible, so it is necessary to adjust the constraints to rebuild the feasible region.

$$\begin{aligned} \min_{\varepsilon_1,\varepsilon_2,\varepsilon_3,\varepsilon_4} \; & J_3 = w_1\varepsilon_1 + w_2\varepsilon_2 + w_3\varepsilon_3 + w_4\varepsilon_4 \\ s.t. \; & f(\hat{x}, \hat{y}, \hat{p}, \hat{d}, u) = 0 \\ & u_{LL} - \varepsilon_1 \le u \le u_{HL} + \varepsilon_2 \\ & y_{LL} - \varepsilon_3 \le \hat{y} \le y_{HL} + \varepsilon_4 \\ & u_{LLL} \le u \le u_{HHL} \\ & y_{LLL} \le \hat{y} \le y_{HHL} \end{aligned} \tag{11}$$

B. THE TARGET TRACKING OF SSTO

Because the optimization model and period of RTO are different from that of the dynamic control layer, the expected values $y_{t,RTO}, u_{t,RTO}$ of the RTO are usually not directly transferred to the dynamic control layer as dynamic setpoints. It is necessary to recalculate the steady-state operating setpoints $y_{t,SSTO}, u_{t,SSTO}$ through SSTO in combination with the current actual situation of the system and the adopted nonlinear model. The target tracking of SSTO problem is shown in equation 12.

$$\begin{aligned} \min_{u,\hat{y}} \; & J_4 = \left(\left\| u - u_{t,RTO} \right\|_R^2 + \left\| \hat{y} - y_{t,RTO} \right\|_Q^2 \right) \\ s.t. \; & f(\hat{x}, \hat{y}, \hat{p}, \hat{d}, u) = 0 \\ & u_{LL} \le u \le u_{HL} \\ & y_{LL} \le \hat{y} \le y_{HL} \end{aligned} \tag{12}$$

C. THE ECONOMIC OPTIMIZATION OF SSTO

SSTO not only has the requirement of tracking RTO optimization target but also has the ability of self-optimization in operation horizon. In other words, according to the process requirements, automatic optimization is carried out near the steady-state target value to find the best process setpoint. Its inherent meaning is to maximize the benefit or minimize the cost caused by the change of control input and controlled output; the first task is to standardize the benefit or cost generated by the unit change of control input, then use the standardized parameter $c^T = \begin{bmatrix} c_1 & c_2 & c_3 \end{bmatrix}$ to represent the benefit or cost of each control input variable, and use the $\pm$ symbol to distinguish the cost and benefit, $+$ represents a cost, $-$ represents a benefit, so the objective function should be minimized. The economic optimization of SSTO problem is shown in equation 13.

$$\begin{aligned} \min_{u,\hat{y}} \; & J_5 = -c_1 w + c_2 T_{pout} + c_3 (T_{c1} + T_{c2}) \\ s.t. \; & f(\hat{x}, \hat{y}, \hat{p}, \hat{d}, u) = 0 \\ & u_{LL} \le u \le u_{HL} \\ & y_{LL} \le \hat{y} \le y_{HL} \end{aligned} \tag{13}$$

D. COORDINATION BETWEEN SSTO FEASIBILITY AND ECONOMIC OPTIMIZATION

From the above SSTO economic optimization, it can be seen that the system optimization feasibility is the necessary condition for the system optimization control when dealing with the complex system optimization control. The following two cases are divided to analyze the relationship between the feasibility and the target coordination.

(1) If SSTO has an optimal feasible region, but when the feasible region of the system is far away from the expected target, the objective function J value will be tremendous from the economic optimization, which shows that even if there is a broader feasible region, it is not necessarily able to get the optimization results satisfactory to users. So, in this case, for the SSTO, the system's feasibility is no longer the only necessary condition for system optimization. On the one hand, if the system still has the remaining degrees of freedom (the adjustability of constraints), we should further use these degrees of freedom to adjust the feasible space of the system to the desired setpoint of the target; on the other hand, we can also soften the target while relaxing the constraints.

(2) When SSTO is not feasible, the optimization problem must be made feasible to coordinate the objectives. It is necessary to construct a feasible region through soft constraint adjustment. For SSTO, it is necessary to take economic optimization into account while optimizing the feasible region's design. Because the feasible region formed by u and $\hat{y}$ constraints is a polyhedral shape, the feasible region reconstructed by constraint adjustment does not necessarily approach to the direction of making the economic optimization goal smaller, which may lead to the optimization results not satisfactory to users. Therefore, when the feasible region of the optimization problem does not exist, we need to adjust the constraints, rebuild the feasible region, and take into account the system's economic optimization.

Therefore, when the feasible region of SSTO is not feasible, or the feasible space of the system is far away from the expected target, it is necessary to adjust the constraints of the system properly to obtain an optimal value satisfying the user.

The coordination and optimization problem is shown in Equation 14, and the second half of object J reflects the economic benefits. If loosening the constraint bound will increase economic benefits, the bound will be adjusted accordingly, and not all soft constraints can be coordinated.

$$\begin{aligned} \min_{\varepsilon_1,\varepsilon_2,\varepsilon_3,\varepsilon_4,u,\hat{y}} \; & J_6 = w_1\varepsilon_1 + w_2\varepsilon_2 + w_3\varepsilon_3 + w_4\varepsilon_4 \\ & - c_1 w + c_2 T_{pout} + c_3(T_{c1} + T_{c2}) \\ s.t. \; & f(\hat{x}, \hat{y}, \hat{p}, \hat{d}, u) = 0 \\ & u_{LL} - \varepsilon_1 \le u \le u_{HL} + \varepsilon_2 \\ & y_{LL} - \varepsilon_3 \le \hat{y} \le y_{HL} + \varepsilon_4 \\ & u_{LLL} \le u \le u_{HHL} \\ & y_{LLL} \le \hat{y} \le y_{HHL} \end{aligned} \tag{14}$$

V. PROPOSED TWO-LAYERED MODEL PREDICTIVE CONTROL STRATEGY

In this section, we introduce MPC and zone MPC (ZMPC). The MPC layer is responsible for the dynamic tracking control of the optimal setpoints [21]. The ZMPC sacrifices some secondary output variables' control requirements to ensure that the main output variables can reach the set value target with limited degrees of freedom [24], [27]–[29]. RTO, SSTO, and MPC structure considered in this work are represented in figure 3.

A. MPC STRUCTURE INTEGRATED WITH SSTO

The two-layer MPC not only keeps the advantages of predictive control but also adds the SSTO layer to recalculate the optimal steady-state output and the input value of the system at each sampling time, to prevent the disturbance entering the system at any time or the input of the operator from changing the optimal steady-state input and output of the system. The dynamic control layer is responsible for the dynamic tracking control of the optimal setpoints. Since the disturbance and the deviation between the predicted output and the measured output are considered in the SSTO, the dynamic control can completely track the target and realize offset free control. The optimal input sequence is obtained from equation 15 of the dynamic optimization problem.

$$\begin{aligned} \min_{u} \; & J_7 = \left(\hat{y} - y_t\right)^T W_t \left(\hat{y} - y_t\right) + \hat{y}^T w_y + u^T w_u \\ & + \Delta u^T W_{\Delta u} \Delta u \\ s.t. \; & 0 = f\left(\frac{d\hat{x}}{dt}, \hat{x}, \hat{y}, \hat{p}, \hat{d}, u\right) \\ & 0 = g(\hat{x}, \hat{y}, \hat{p}, \hat{d}, u) \\ & 0 \le h(\hat{x}, \hat{y}, \hat{p}, \hat{d}, u) \\ & \tau_c \frac{dy_t}{dt} + y_t = sp \end{aligned} \tag{15}$$

In the above optimization, $\hat{x}$, $\hat{y}$, $\hat{p}$ and $\hat{d}$ represent the state and parameter estimate from NMHE. J_7 represents minimized objective function result; y_t represents desired trajectory target ($y_{t,RTO}$, $y_{t,SSTO}$); W_t represents penalty outside reference trajectory; w_u and w_y represent the weights on input and output; Δu represents manipulated variable change; $W_{\Delta u}$ represents manipulated variable movement penalty; *sp* represents operating setpoint; τ_c represents time constant of desired controlled variable response. In the dynamic control, three goals are achieved: (1) the future *CV* is as close to y_t as possible, (2) the drastic change of *MV* is restrained.

B. NONLINEAR CONTROL OF NONSQUARE MULTIVARIABLE SYSTEM

The general description is as follows: The nonlinear system is square (the number of control input variables is equal to the number of controlled output variables), and its process steady-state gain matrix exists and is reversible. After the output target is given, it means that the control input target is also determined simultaneously. The steady-state values of input and output are compatible. Nonsquare systems are divided into two cases: (1) The systems with a degree of freedom $D > 0$ (the number of control input variables is higher than the number of output variables), and a given output target can have many types of control input combinations corresponding to it. (2) For a system with a degree of freedom $D < 0$ (the number of control input variables is less than the number of output variables), the given output target is often unreachable, and the process has a steady-state error.

Consider the cut tobacco drying process nonlinear system with 4 states, 2 inputs, and 4 outputs. Based on the nonlinear system's input/output linearization, the relationship between the steady-state input and the steady-state output value of the nonsquare system is analyzed. As shown in equation 16, L_u is the characteristic matrix of the system, Ξ is the augmented matrix of the system. For the system with a degree of freedom $D < 0$, the root cause of the possible incompatibility of the steady-state solution lies in the fact that $rank(L_u) < rank(\Xi)$. It is known theoretically that if y_t belongs to the column space of L_u, then $L_u u_t = y_t$ must be compatible, that is, $rank(L_u) = rank(\Xi)$, indicating that the steady-state solution of the control input is unique at this time. It can be seen that if we can find y_t, which makes $rank(L_u) = rank(\Xi)$, then the problem of compatibility and uniqueness of the steady-state solution of the system will be solved at the same time. The key to ensuring that y_t is an element in the column space of L_u, but y_t itself is not unique.

$$\begin{aligned} L_u &= \begin{bmatrix} L_{11} & L_{12} & \cdots & L_{1m} \\ \vdots & \vdots & \vdots & \vdots \\ L_{p1} & L_{p2} & \vdots & L_{pm} \end{bmatrix}_{p\times m} \\ \Xi &= \begin{bmatrix} L_{11} & L_{12} & \cdots & L_{1m} & y_{t,1} \\ \vdots & \vdots & \vdots & \vdots & \vdots \\ L_{p1} & L_{p2} & \cdots & L_{pm} & y_{t,m} \end{bmatrix}_{p\times(m+1)} \\ L_u u_t &= y_t \end{aligned} \tag{16}$$

According to the theory, the primary reason why the system with $D < 0$ is usually uncontrollable is that the setpoint is not given reasonably. The way to solve the control problem

of the system is as follows: (1) select a set of more reasonable (that is, make the input-output steady-state relationship equation have a solution). (2) Reduce the number of equations, so that the number of equations (the number of outputs) is equal to the number of unknown variables (the number of inputs), or make the number of equations less than the number of unknown variables constitute a sub definite equation group, usually with solutions, and whether there are array solutions.

The first method to solve the system with a degree of freedom $D < 0$ is the two-layered model predictive control with integrated steady-state target optimization (SSTO). Based on the multivariable predictive control, a steady-state target optimization layer is introduced to ensure that the steady-state solution (u_t, y_t) of the optimal control input and controlled output is uniquely determined. The second method is the zone control. Its essence is: for the control of the system with a degree of freedom $D < 0$, the zone control strategy is adopted for some outputs, that is, to give up the setpoint of this part of the output, that is, to reduce the number of steady-state equations, to obtain unique solutions, or even infinite solutions (the number of solutions is related to the number of relaxed outputs of the zone control strategy), to eliminate the steady-state error of the output.

The optimal objective function of the zone control strategy is the L1-Norm objective (as in Equation 17). By sacrificing some secondary output variables' control requirements, the limited degrees of freedom can ensure that the main output variables can achieve the setpoint objective. Another feature of zone control is the way to deal with system disturbances. In extreme cases (all outputs use zone control), the controller may not generate any action for disturbance in the entry process. For a process that uses a hybrid control mode (partial output is setpoint control, and part output is zone control, which is also common in practice), the controller can respond to disturbances with minimal controller action. The L1-Norm zone MPC gives an intuitive way to manage these tradeoffs for problems with security, environment, economy, and other competing priorities.

$$
\begin{aligned}
\min_{u}\ & J_8 = w_{hi}^T e_{hi} + w_{lo}^T e_{lo} + \hat{y}^T w_y + u^T w_u \\
& \quad + w_{\Delta u}^T (\Delta u_U + \Delta u_L) \\
s.t.\ & 0 = f\left(\frac{d\hat{x}}{dt}, \hat{x}, \hat{y}, \hat{p}, \hat{d}, u\right) \\
& 0 = g(\hat{x}, \hat{y}, \hat{p}, \hat{d}, u) \\
& 0 \le h(\hat{x}, \hat{y}, \hat{p}, \hat{d}, u) \\
& \tau_c \frac{dy_{t,hi}}{dt} + y_{t,hi} = sp_{hi} \\
& \tau_c \frac{dy_{t,l0}}{dt} + y_{t,lo} = sp_{lo} \\
& e_{hi} \ge \hat{y} - y_{t,hi} \\
& e_{l_0} \ge y_{t,lo} - \hat{y} \\
& \Delta u_U \ge u_i - u_{i-1} \\
& \Delta u_L \ge u_{i-1} - u_i
\end{aligned}
$$

$$
e_{hi}, e_{l_0}, \Delta u_U, \Delta u_L \ge 0 \tag{17}
$$

In the above optimization, $\hat{x}$, $\hat{y}$, $\hat{p}$ and $\hat{d}$ represent the state and parameter estimate from NMHE. J_8 represents minimized objective function result; w_{hi}^T and w_{lo}^T represent penalty outside reference trajectory; e_{hi} and e_{lo} represent upper and lower error outside dead-band; w_u and w_y represent the weight on input and output; $w_{\Delta u}^T$ represents manioulated variable movement penalty; Δu_U and Δu_L represent upper and lower manipulated variable change; sp_{hi} and sp_{lo} represent upper and lower bounds to final setpoint dead-band; $y_{t,hi}$ and $y_{t,lo}$ represent upper and lower bounds to desired trajectory target.

VI. SIMULATION RESULT

In this section, we apply the proposed SSTO-MPC and RTO zone MPC (RTO-ZMPC) to the cut tobacco drum dryer system and compare its performance with the RTO-MPC. The optimization problems (NMHE, SSTO-MPC, RTO-MPC, and RTO-ZMPC) are solved using IPOPT in Matlab based on APMonitor [24].

A. SYSTEM PARAMETERS AND CONSTRAINTS

For the cut tobacco drum dryer system in equation 6, model parameters used in the simulations are given in Table 1. The lower and upper limits of the operation constraints of manipulated inputs are $u_{LL} = \begin{bmatrix} 0 & 0 \end{bmatrix}^T$ and $u_{HL} = \begin{bmatrix} 200 & 200 \end{bmatrix}^T$, respectively. The lower and upper bounds of the engineering constraints of manipulated inputs are $u_{LLL} = \begin{bmatrix} 0 & 0 \end{bmatrix}^T$ and $u_{HHL} = \begin{bmatrix} 250 & 250 \end{bmatrix}^T$, respectively. The lower and upper limits of the changing rates of the two manipulated inputs are $\Delta u_{min} = \begin{bmatrix} 10 & 10 \end{bmatrix}^T$ and $\Delta u_{max} = \begin{bmatrix} 100 & 100 \end{bmatrix}^T$, respectively. The lower and upper limits of the operation constraints of system outputs are $y_{LL} = \begin{bmatrix} 0.13 & 130 & 20 & 100 \end{bmatrix}^T$ and $y_{HL} = \begin{bmatrix} 0.16 & 170 & 100 & 120 \end{bmatrix}^T$, respectively. The lower and upper bounds of the engineering constraints of system outputs are $y_{LLL} = \begin{bmatrix} 0.13 & 100 & 20 & 100 \end{bmatrix}^T$ and $y_{HHL} = \begin{bmatrix} 0.20 & 200 & 105 & 150 \end{bmatrix}^T$, respectively. The lower and upper limits of the three system parameters are $p_{min} = \begin{bmatrix} 0 & 0 & 0 \end{bmatrix}^T$ and $p_{max} = \begin{bmatrix} 200 & 50 & 1000 \end{bmatrix}^T$, respectively.

B. SYSTEM PARAMETERS AND STATES ESTIMATION USING NMHE

First, the state and parameter estimation performance of the NMHE scheme introduced in Section 3 is illustrated. It is assumed that the three outputs (T_{dryer}, T_{pout} and T_1) are measured every $\Delta T = 1s$ and the measurements are immediately available to the state estimator. First of all, the estimator must predict the outlet moisture content of cut tobacco w, because there is no direct measurement of this output variable. Secondly, three thermal conductivity $keff$, $keff1$ and $keff2$ need to be predicted. We consider that the system is at initially a zero state x_0 and the corresponding initially input is $u_0 = \begin{bmatrix} 100 & 130 \end{bmatrix}^T$. The choice of NMHE window length N is based on extensive simulation. The simulation results show

that when N is greater than 6, the estimation performance is not significantly improved. Therefore, N is chosen as 10. In order to illustrate the estimation performance of NMHE, a set of step input signals ($u(1:19) = \begin{bmatrix}100 & 130\end{bmatrix}^T$ and $u(20:90) = \begin{bmatrix}130 & 150\end{bmatrix}^T$) are applied to the nonlinear cut tobacco drum dryer system. Figure 4 shows the results of the parameters and states estimation. For this application, the results indicate that NMHE provides accurate estimates of three thermal conductivity and four states, especially when the cut tobacco outlet moisture content is not measurable; it is also estimated accurately.

C. OPTIMAL OPERATING SETPOINTS OF SSTO AND RTO

The proposed SSTO approach was applied in the control of the cut tobacco drying process. The SSTO economic function to be used in the simulation is presented in equation 14 and RTO economic function in equation 10. In table 2, four different optimum operating setpoints are displayed, which were obtained through the solution of the RTO and SSTO, for corresponding weight values of c^T. The first and second operating setpoints are obtained in the nominal condition, and the third and fourth operating setpoints are obtained in the disturbance condition. In the disturbance condition, the SSTO problem is not feasible, so it is necessary to relax the operation constraints (u) to find a feasible solution. The optimal operating setpoints of SSTO and RTO are sent downwards to the MPC control structure to validate our proposed approach.

D. RESULTS OF OPTIMAL OPERATING SETPOINTS-TRACKING CAPABILITY TESTS

The nonlinear system of cut tobacco drying has four states: a nonsquare system and two inputs and four outputs. The optimal operating setpoints under under different system conditions have been transmitted to the lower control structure through SSTO and RTO. Therefore, this section first verifies the tracking capability of the proposed SSTO-MPC and RTO-MPC; it is assumed that the entire state vector is measured and available to the controllers.

Simulation is carried out in two typical cases, the first of which is system simulation in a nominal case. First simulation, the weight coefficient of RTO and SSTO objective functions is $c^T = \begin{bmatrix}1 & 1 & 1 & 1\end{bmatrix}$ and corresponding optimal operating setpoints of SSTO and RTO are $y_{t,SSTO} = \begin{bmatrix}0.1535 & 130 & 58.8876 & 100\end{bmatrix}^T$ and $y_{t,RTO} = \begin{bmatrix}0.1584 & 131.2529 & 58.0798 & 100\end{bmatrix}^T$, respectively. The weighting matrix coefficient of MPC objective function is $W_t = diag\left(\begin{bmatrix}30 & 20 & 20 & 10\end{bmatrix}\right)$ and represents penalty outside reference trajectory. $W_{\Delta u}$ represents manipulated variable movement penalty, here we choose as $W_{\Delta u} = diag\left(\begin{bmatrix}200 & 200\end{bmatrix}\right)$. SSTO-MPC and RTO-MPC track the optimal operating setpoints in closed-loop simulation as shown in figure 5. In figure 5, $e1 = w_{sp} - w$ represents the outlet moisture error of cut tobacco. In the whole system, the outlet moisture content of the cut tobacco is the most critical controlled output variable, which is directly related to the quality of cigarette products. It can be seen from figure 5 that RTO-MPC has static error control, and SSTO-MPC can well control each output variable without static error.

In the second simulation, when the weight coefficient of the objective function of RTO and SSTO is changed, i.e., $c^T = \begin{bmatrix}-1 & 1 & 1 & 1\end{bmatrix}$ and corresponding optimal operating setpoints of SSTO and RTO are $y_{t,SSTO} = \begin{bmatrix}0.1444 & 141.1501 & 56.4244 & 100\end{bmatrix}^T$ and $y_{t,RTO} = \begin{bmatrix}0.16 & 135.0332 & 56.2106 & 100\end{bmatrix}^T$, respectively. The weighting matrices W_t and $W_{\Delta u}$ are selected to be the same as the first simulation. SSTO-MPC and RTO-MPC track the optimal operating setpoints in the closed-loop simulation, as shown in figure 6. It can be seen from figure 6 that RTO-MPC still has a small static error, while SSTO-MPC is still no static error control.

In the second case, we consider a disturbance in the system, either from upstream equipment or the equipment itself. Here, we assume that the moisture and temperature at the inlet of the cut tobacco from the upstream equipment fluctuate, i.e. $w_{in} = 0.20$, $T_{pin} = 35$; the air temperature at the inlet of the heater changes twice as much, i.e. $T_{in} = 40$. Third simulation, the weight coefficient of RTO and SSTO objective functions is $c^T = \begin{bmatrix}1 & 1 & 1 & 1\end{bmatrix}$ and corresponding optimal operating setpoints of SSTO and RTO are $y_{t,SSTO} = \begin{bmatrix}0.16 & 134.5834 & 61.3004 & 100\end{bmatrix}^T$ and $y_{t,RTO} = \begin{bmatrix}0.16 & 130 & 58.6144 & 100\end{bmatrix}^T$, respectively. The weighting matrices W_t and $W_{\Delta u}$ are selected to be the same as the first simulation. SSTO-MPC and RTO-MPC track the optimal operating setpoints in the closed-loop simulation, as shown in figure 7. It can be seen from figure 7 that when there is a disturbance in the system, RTO-MPC still has static error control, which cannot overcome the shortcomings of the control of the nonsquare system; at the same time, the moisture of the cut tobacco outlet exceeds the operational constraints of the output variable, which affects the quality of subsequent products. SSTO-MPC achieves the error-free tracking of output variables by relaxing the constraints of operating variables.

It can be seen from the simulation that compared with RTO-MPC, the proposed SSTO-MPC has better tracking performance for the nonsquare system of the nonlinear cut tobacco drying process.

E. ZONE CONTROL OF THE NONSQUARE SYSTEM

In the cut tobacco drying process, the primary task is to meet the outlet moisture content of cut tobacco. Under the condition of reducing the operation cost, as long as the cut tobacco outlet temperature, drum dryer temperature, and hot air temperature meet the process requirements, energy consumption can be saved. The second control strategy for nonsquare systems is zone MPC. We set a dead band zone for drum dryer temperature T_{dryer} and hot air temperature T_1 to meet the process requirements. The primary purpose of setting the dead band zone is to reject the measurement error and stabilize the parameter estimation. A unique feature of

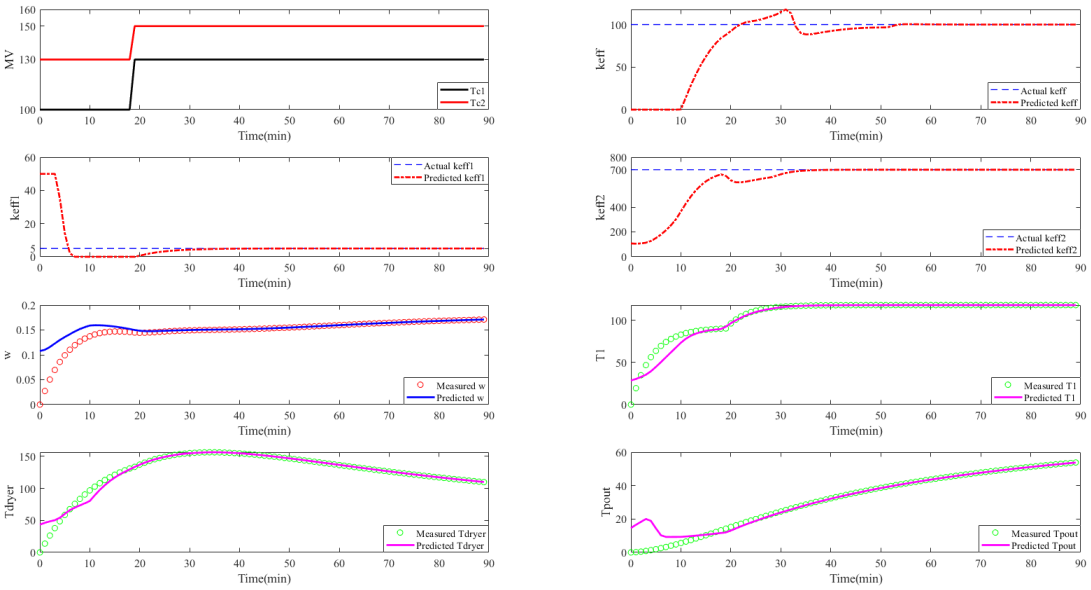

FIGURE 4. Trajectories of the actual states and parameters, and states and parameters estimate by the NMHE.

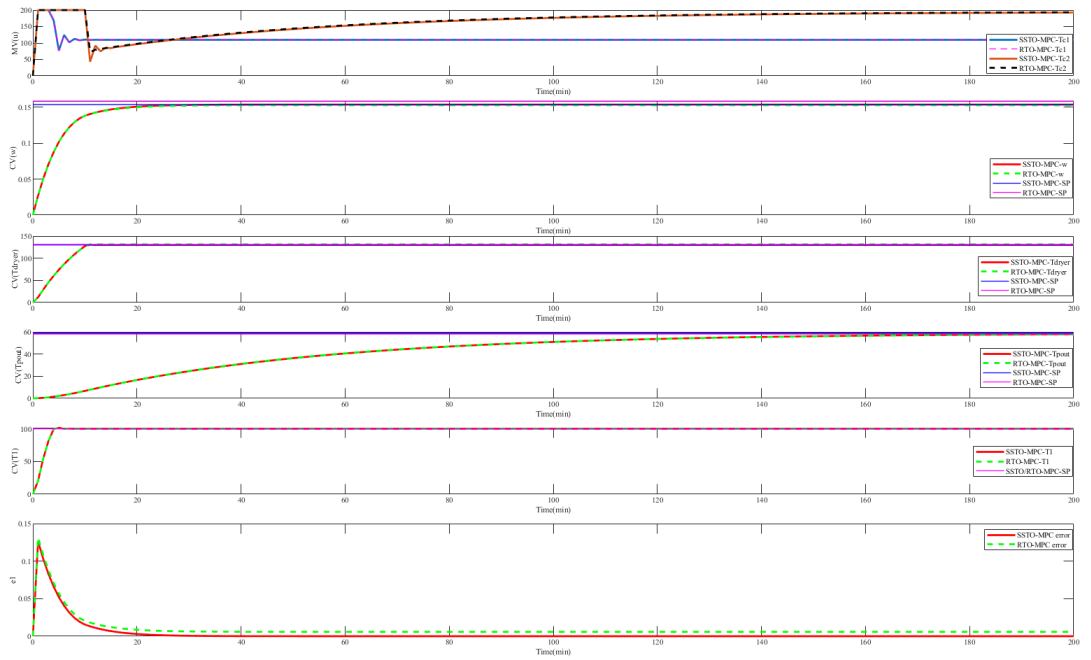

FIGURE 5. Under the nominal condition, SSTO-MPC and RTO-MPC track the optimal operating setpoints in the closed-loop simulation.

the zone MPC is that a dead band zone or no penalty zone is added to the measured value without causing any loss. Only when the model prediction exceeds this dead band zone will the optimizer change the parameters to modify the model. This setting reduces the controller actions to a certain extent, achieving cost savings, and optimizing economic goals.

For the proposed RTO zone MPC (RTO-ZMPC), In the optimization problem equation 17, w_{hi}^T and w_{lo}^T represent penalty outside reference trajectory, here we choose as: $w_{hi}^T = \begin{bmatrix} 30 & 20 & 20 & 10 \end{bmatrix}$, $w_{lo}^T = \begin{bmatrix} 30 & 20 & 20 & 10 \end{bmatrix}$. w_u and w_y choose as the identity matrix. $W_{\Delta u}$ is selected to be the same as the first simulation. In the cut tobacco drying process, the primary task is to meet the outlet moisture content of cut tobacco. We set a dead band zone for drum dryer temperature T_{dryer} and hot air temperature T_1 to meet the process requirements and the outlet moisture content setpoint w and outlet

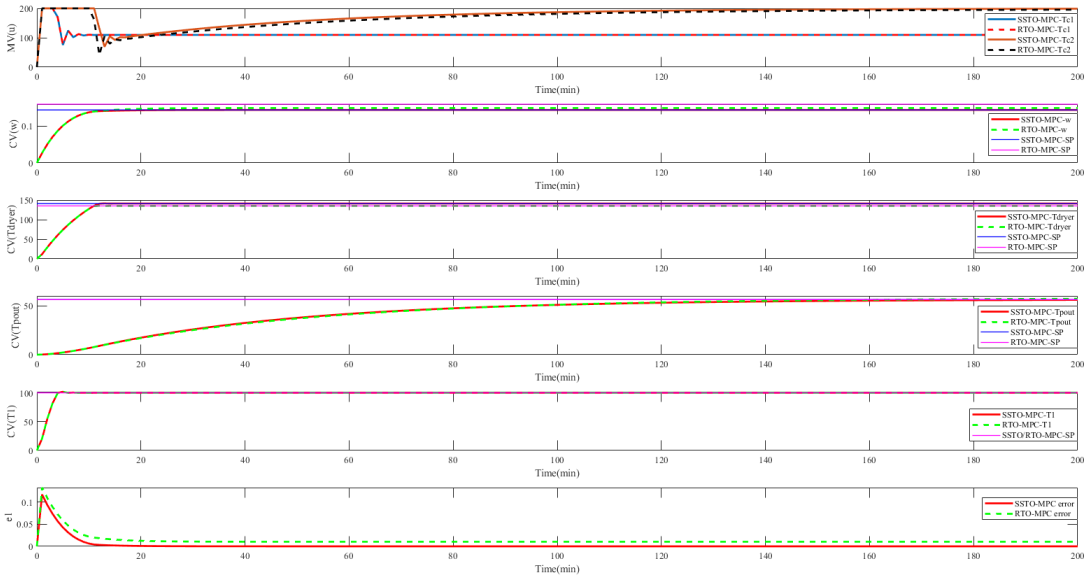

FIGURE 6. Under the nominal condition, SSTO-MPC and RTO-MPC track the optimal operating setpoints in the closed-loop simulation.

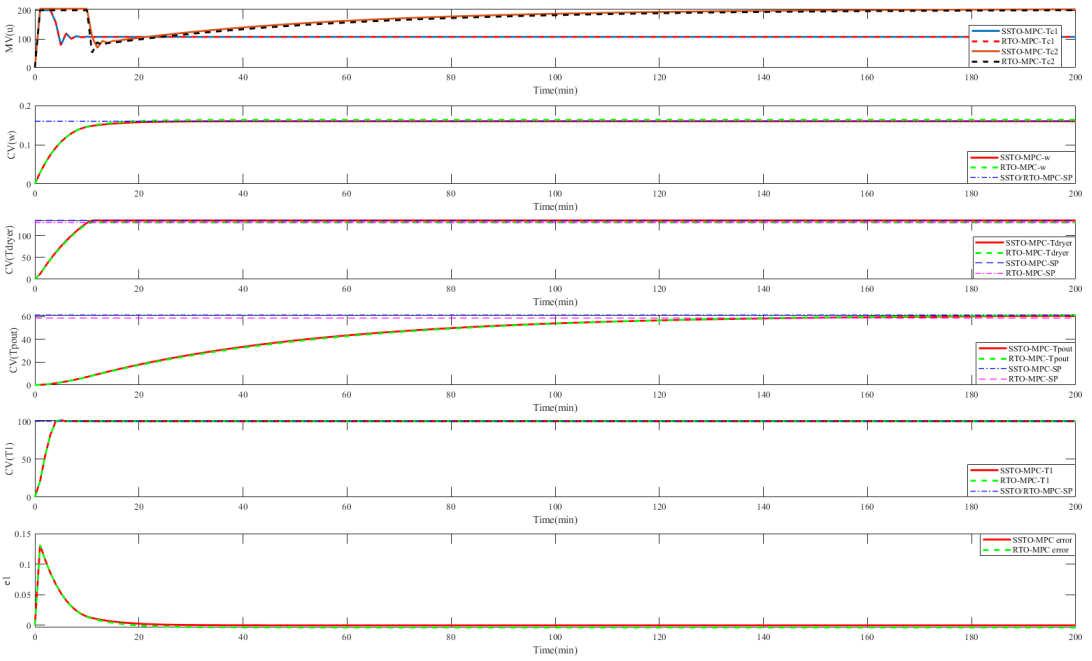

FIGURE 7. Under the disturbance condition, SSTO-MPC and RTO-MPC track the optimal operating setpoints in the closed-loop simulation.

TABLE 2. Optimal operating setpoints of the cut tobacco dryer.

Situation and weight	RTO and SSTO	T_{c1}	T_{c2}	w	T_1	T_{pout}	T_{dryer}	ε_1	ε_2	obj
Nominal condition $c^T = [\ 1 \quad 1 \quad 1\ ]$	RTO	109.5768	200	0.1584	100	58.0798	131.2529	–	–	1.0921
	$SSTO$	109.5768	194.8092	0.1535	100	58.8876	130	–	–	1.2986
Nominal condition $c^T = [\ -1 \quad 1 \quad 1\ ]$	RTO	109.5768	200	0.16	100	56.2106	135.0332	–	–	3.2505
	$SSTO$	109.5768	200	0.1444	100	56.4244	141.1501	–	–	3.1556
Disturbance condition $c^T = [\ 1 \quad 1 \quad 1\ ]$	RTO	107.1826	200	0.16	100	58.6144	130	–	–	1.2686
	$SSTO$	107.1826	204.9633	0.16	100	61.3004	134.5834	0	4.9633	1.3270
Disturbance condition* $c^T = [\ -1 \quad 1 \quad 1\ ]$	RTO	107.1826	200	0.16	100	43.4009	165.6059	–	–	3.1658
	$SSTO$	107.1826	217.4481	0.13	100	55.3745	162.5643	0	17.4481	3.1278

* indicates that this set of optimized operating setpoints are used for section E simulation.

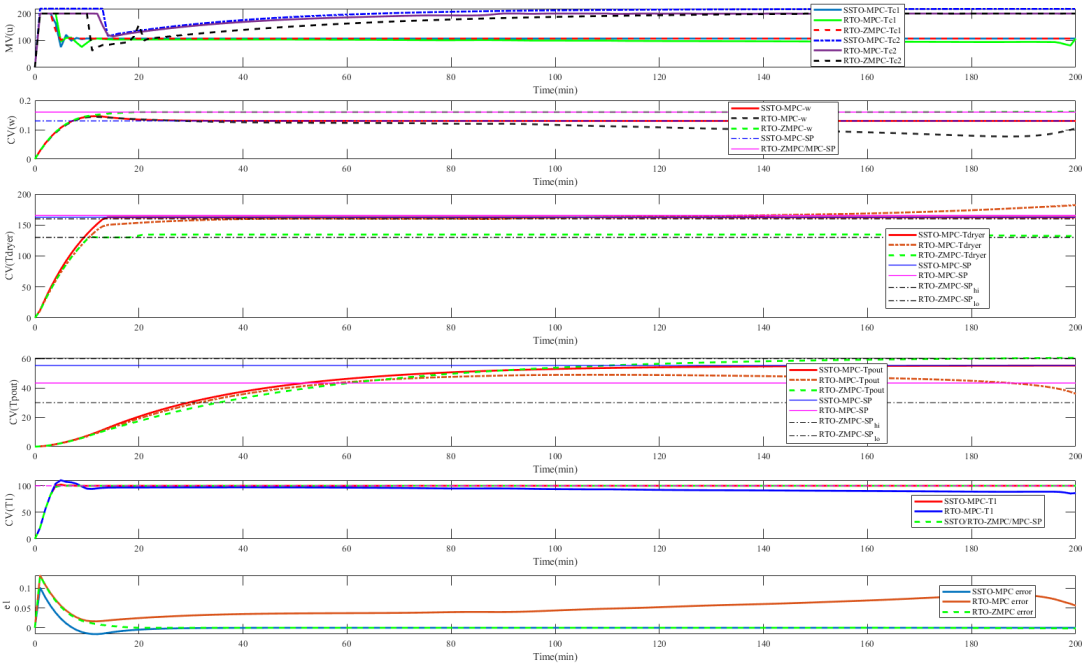

FIGURE 8. Under the disturbance condition, SSTO-MPC, RTO-MPC, and RTO-ZMPC track the optimal operating setpoints in the closed-loop simulation.

temperature of cut tobacco T_{pout} are same as RTO. sp_{hi} and sp_{lo} represent upper and lower bounds to final setpoint deadband zone, here we choose as: $sp_{hi} = \begin{bmatrix} 0.16 & 160 & 60 & 110 \end{bmatrix}$, $sp_{lo} = \begin{bmatrix} 0.16 & 150 & 20 & 100 \end{bmatrix}$. The simulation conditions are the same as the third simulation, the weight coefficient of RTO and SSTO objective functions is $c^T = \begin{bmatrix} -1 & 1 & 1 & 1 \end{bmatrix}$ and corresponding optimal operating setpoints of SSTO and RTO are $y_{t,SSTO} = \begin{bmatrix} 0.13 & 162.5643 & 55.3745 & 100 \end{bmatrix}^T$ and $y_{t,RTO} = \begin{bmatrix} 0.16 & 165.6059 & 43.4009 & 100 \end{bmatrix}^T$, respectively. SSTO-MPC, RTO-MPC, and RTO-ZMPC track the optimal operating setpoints in the closed-loop simulation, as shown in figure 8. As can be seen from figure 8, RTO-ZMPC is also an effective control strategy for nonsquare systems, which has good tracking performance and realizes the controller's minimum action economy. However, the selection of the dead band zone for RTO-ZMPC is more based on engineering practice, while SSTO-MPC is a more desirable control strategy to obtain exact optimal operation setpoints based on strict optimization problems.

VII. CONCLUSION

This article proposes a double-layer MPC (SSTO-MPC) control strategy for the nonsquare system of the nonlinear tobacco drying process, which overcomes the shortcomings of traditional MPC (RTO-MPC) in static error control of the nonsquare system. Simulation results show that SSTO-MPC has better tracking ability and disturbance suppression ability than RTO-MPC. At the same time, the addition of the SSTO layer makes MPC have a more flexible framework. Compared with RTO-ZMPC, SSTO-MPC has a more rigorous theoretical optimization operation setpoint, and the implementation is more scientific and reasonable. Overall, the proposed double-layer MPC (SSTO-MPC) provides an attractive control alternative to the conventional tracking MPC.

CONFLICTS OF INTEREST

The authors declare no conflicts of interest.

DATA AVAILABILITY

The data used to support the findings of this study are available from the corresponding author upon request.

REFERENCES

[1] P. Dufour, "Control engineering in drying technology: Review and trends," *Drying Technol.*, vol. 24, no. 7, pp. 889–904, Aug. 2006.
[2] G. R. Luz, W. A. dos Santos Conceição, L. M. de Matos Jorge, P. R. Paraíso, and C. M. G. Andrade, "Dynamic modeling and control of soybean meal drying in a direct rotary dryer," *Food Bioproducts Process.*, vol. 88, nos. 2–3, pp. 90–98, Jun. 2010.
[3] H. Didriksen, "Model based predictive control of a rotary dryer," *Chem. Eng. J.*, vol. 86, nos. 1–2, pp. 53–60, Feb. 2002.
[4] H. Abbasfard, H. H. Rafsanjani, S. Ghader, and M. Ghanbari, "Mathematical modeling and simulation of an industrial rotary dryer: A case study of ammonium nitrate plant," *Powder Technol.*, vol. 239, pp. 499–505, May 2013.
[5] W. K. Zhu, L. Wang, K. Duan, L. Y. Chen, and B. Li, "Experimental and numerical investigation of the heat and mass transfer for cut tobacco during two-stage convective drying," *Drying Technol.*, vol. 33, no. 8, pp. 907–914, Jun. 2015.
[6] P. C. Panchariya, D. Popovic, and A. L. Sharma, "Thin-layer modelling of black tea drying process," *J. Food Eng.*, vol. 52, no. 4, pp. 349–357, May 2002.
[7] A. Iguaz, H. Budman, and P. L. Douglas, "Modelling and control of an alfalfa rotary dryer," *Drying Technol.*, vol. 20, no. 9, pp. 1869–1887, Jan. 2002.

[8] Y. Rousselet and V. K. Dhir, "Numerical modeling of a co-current cascading rotary dryer," *Food Bioproducts Process.*, vol. 99, pp. 166–178, Jul. 2016.
[9] N. Daraoui, P. Dufour, and H. Hammouri, "Benefits in using model based predictive control during drying and lyophilisation," in *Proc. 3rd Eur. Drying Conf. Joint Conf. Eur. Fed. Chem. Eng. (EFCE) Drying Working Party, Assoc. Française Séchage dans l'Industrie et l'Agricult. (AFSIA)*, in Cahier de l'AFSIA, vol. 23, no. 1. Lyon, France:, May 2009, pp. 100–101.
[10] N. Colak and A. Hepbasli, "A review of heat pump drying: Part 1—Systems, models and studies," *Energy Convers. Manage.*, vol. 50, no. 9, pp. 2180–2186, Sep. 2009.
[11] T. Defraeye, "Advanced computational modelling for drying processes—A review," *Appl. Energy*, vol. 131, pp. 323–344, Oct. 2014.
[12] N. J. B. McFarlane and D. M. Bruce, "A cost function for continuous-flow grain drying and its use in control," *J. Agricult. Eng. Res.*, vol. 65, no. 1, pp. 63–75, Sep. 1996.
[13] R. Dhib, N. Thérien, and A. D. Broadbent, "Model-based multivariable control of the drying of a thin sheet of fibres in a continuous infrared dryer," *Can. J. Chem. Eng.*, vol. 77, no. 5, pp. 1055–1064, Oct. 1999.
[14] I. Alvarez-López, O. Llanes-Santiago, and J. L. Verdegay, "Drying process of tobacco leaves by using a fuzzy controller," *Fuzzy Sets Syst.*, vol. 150, no. 3, pp. 493–506, Mar. 2005.
[15] V. M. Cristea, M. Baldea, and S. P. Agachi, "Model predictive control of an industrial dryer," in *Computer Aided Chemical Engineering* (European Symposium on Computer Aided Process Engineering), vol. 8, S. Pierucci, Ed. Amsterdam, The Netherlands: Elsevier, Jan. 2000, pp. 271–276.
[16] H. Abukhalifeh, R. Dhib, and M. E. Fayed, "Model predictive control of an infrared-convective dryer," *Drying Technol.*, vol. 23, no. 3, pp. 497–511, Mar. 2005.
[17] L. N. Petersen, N. K. Poulsen, H. H. Niemann, C. Utzen, and J. B. Jorgensen, "Application of constrained linear MPC to a spray dryer," in *Proc. IEEE Conf. Control Appl. (CCA)*, Oct. 2014, pp. 2120–2126.
[18] L. N. Petersen, N. K. Poulsen, H. H. Niemann, C. Utzen, and J. B. Jørgensen, "Comparison of three control strategies for optimization of spray dryer operation," *J. Process Control*, vol. 57, pp. 1–14, Sep. 2017.
[19] R. Findeisen and F. Allgöwer, "An introduction to nonlinear model predictive control," in *Proc. 21st Benelux Meet. Syst. Control*, Jan. 2002, pp. 1–23.
[20] D. Q. Mayne, "Model predictive control: Recent developments and future promise," *Automatica*, vol. 50, no. 12, pp. 2967–2986, Dec. 2014.
[21] A. Emhemed and R. Mamat, "Model predictive control: A summary of industrial challenges and tuning techniques," *Int. J. Mechtron., Elect. Comput. Technol.*, vol. 10, pp. 4441–4459, Jul. 2019.
[22] M. Darby, M. Nikolaou, J. Jones, and D. Nicholson, "Rto—An overview and assessment of current practice," *J. Process Control*, vol. 21, pp. 874–884, Jul. 2011.
[23] B. Chachuat, B. Srinivasan, and D. Bonvin, "Adaptation strategies for real-time optimization," *Comput. Chem. Eng.*, vol. 33, no. 10, pp. 1557–1567, Oct. 2009.
[24] J. D. Hedengren, R. A. Shishavan, K. M. Powell, and T. F. Edgar, "Nonlinear modeling, estimation and predictive control in APMonitor," *Comput. Chem. Eng.*, vol. 70, pp. 133–148, Nov. 2014.
[25] S.-Q. Li and B.-C. Ding, "An overall solution to double-layered model predictive control based on dynamic matrix control," *Acta Automatica Sinica*, vol. 41, pp. 1857–1866, Nov. 2015.
[26] D. E. Kassmann, T. A. Badgwell, and R. B. Hawkins, "Robust steady-state target calculation for model predictive control," *AIChE J.*, vol. 46, no. 5, pp. 1007–1024, May 2000.
[27] S. Liu, Y. Mao, and J. Liu, "Model-predictive control with generalized zone tracking," *IEEE Trans. Autom. Control*, vol. 64, no. 11, pp. 4698–4704, Nov. 2019.
[28] Y. Mao, S. Liu, J. Nahar, J. Liu, and F. Ding, "Soil moisture regulation of agro-hydrological systems using zone model predictive control," *Comput. Electron. Agricult.*, vol. 154, pp. 239–247, Nov. 2018.
[29] Y. Zhang, B. Decardi-Nelson, J. Liu, J. Shen, and J. Liu, "Zone economic model predictive control of a coal-fired boiler-turbine generating system," *Chem. Eng. Res. Des.*, vol. 153, pp. 246–256, Jan. 2020.
[30] C. V. Rao and J. B. Rawlings, "Constrained process monitoring: Moving-horizon approach," *AIChE J.*, vol. 48, no. 1, pp. 97–109, Jan. 2002.
[31] C. V. Rao, J. B. Rawlings, and D. Q. Mayne, "Constrained state estimation for nonlinear discrete-time systems: Stability and moving horizon approximations," *IEEE Trans. Autom. Control*, vol. 48, no. 2, pp. 246–258, Feb. 2003.
[32] J. D. Hedengren, K. V. Allsford, and J. Ramlal, "Moving horizon estimation and control for an industrial gas phase polymerization reactor," in *Proc. Amer. Control Conf.*, New York, NY, USA, Jul. 2007, pp. 1353–1358.
[33] B. J. Spivey, J. D. Hedengren, and T. F. Edgar, "Constrained nonlinear estimation for industrial process fouling," *Ind. Eng. Chem. Res.*, vol. 49, no. 17, pp. 7824–7831, Sep. 2010.
[34] S. M. Safdarnejad, J. R. Gallacher, and J. D. Hedengren, "Dynamic parameter estimation and optimization for batch distillation," *Comput. Chem. Eng.*, vol. 86, pp. 18–32, Mar. 2016.
[35] J. D. Hedengren and A. N. Eaton, "Overview of estimation methods for industrial dynamic systems," *Optim. Eng.*, vol. 18, no. 1, pp. 155–178, Mar. 2017.

ANGANG CHEN received the M.S. degree in 2016. He is currently pursuing the Ph.D. degree with the Control Science and Engineering, Donghua University. His research interests include process control theory and practice, emphasis on model predictive control, advanced control of combined integrating systems, modeling and optimization of chemical processes, and real-time control of chemical processes and energy generation systems.

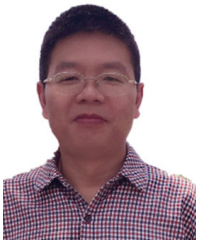

ZHENGYUN REN received the Ph.D. degree from the Department of Automation, Shanghai Jiao Tong University, in 2003. In 2003, he employed at Donghua University, as a Tutor and a Professor. He was a Postdoctoral Researcher with Alberta University, from 2006 to 2007. His current research interests include advanced process control, advanced control of the combined integrating systems, online hysteresis detection, and control, modeling, and optimization of the chemical process, control, and optimization of the tobacco process.

ZHIPING FAN received the M.S. degree from Northwest A&F University, in 2010. She is currently pursuing the Ph.D. degree with the Control Science and Engineering, Donghua University. Since 2013, she has been a Lecturer with Anhui Science and Technology University. Her research interests include advanced process control, advanced control of the combined integrating systems, modeling, and optimization of the chemical process, control, and optimization of the tobacco process.

XUE FENG received the M.S. degree in 2018. She is currently pursuing the Ph.D. degree in control science and engineering with Donghua University. Her research interests include advanced process control, modeling, and optimization of the chemical process.